Antonio Espuña, Moisès Graells and Luis Puigjaner (Editors), Proceedings of the 27th European Symposium on Computer Aided Process Engineering – ESCAPE 27
October 1st - 5th, 2017, Barcelona, Spain

Characterisation of axial dispersion in a Meso-scale Oscillatory Baffled Crystalliser using a Numerical Approach

Emmanuel N. Kimuli[a], Iyke I. Onyemelukwe[a], Brahim Benyahia[a], Chris D. Rielly[a]

[a]*Department of Chemical Engineering, Loughbororough University, Loughborough, Leicestershire, LE11 3TU, UK*
C.D.Rielly@lboro.ac.uk

Abstract

A meso-scale oscillatory baffled crystalliser (meso-OBC) of 5 mm diameter was characterised using Computational Fluid Dynamics (CFD). Residence time distributions (RTD) and axial dispersion coefficients were investigated for a range of oscillation frequencies (2, 6 and 12 Hz), amplitudes (0.5, 1 and 2 mm centre-to-peak) and net flow rates (2 and 5 ml/min) to determine operating conditions that delivered near plug flow behaviour. RTD parameters were fitted to the computed concentration profiles using an axial dispersion model with an imperfect pulse input. The narrowest RTD curve and lowest axial dispersion coefficient was obtained at oscillatory conditions of 6 Hz frequency and 0.5 mm amplitude. The numerical data is validated against experimentally obtained axial dispersion coefficient and the results are in good agreement.

Keywords: Axial dispersion coefficient, CFD, meso-scale oscillatory baffled crystalliser, RTD.

1. Introduction

Improvements to fluid mixing as a direct result of introducing oscillations to net flow in tubes with periodically spaced baffle constrictions is well known and has received wide attention for the past three decades. Brunold et al. (1989) found that interaction between the oscillating fluid and the baffles generated vortices or eddies that increased the radial velocity to have a comparable magnitude to the axial velocity component, hence increasing the intensity and uniformity of mixing within each inter-baffle cell. The assessment of the residence time distribution (RTD) in process unit operations is of paramount importance in their design and operation, as it directly relates to the back-mixing characteristics in the system. There are two main types of RTD achievable in process vessels i.e. very narrow and symmetric distribution, centred about the mean residence time, which is the case in plug flow, where radial mixing dominates over axial mixing; at the other extreme, the RTD is very broad with a long tail, which is characteristic of a continuous stirred tank reactor. In continuous operation of tubular crystallisers, a narrow RTD is preferred, as it is more likely to lead to a narrow crystal size distribution, which has better filtration, isolation and drying characteristics.

Oscillatory baffled reactors (OBR) are tubes or columns with periodically spaced baffle divisions that create equally sized cells; the fluid is subjected to oscillations via means of a piston, diaphragm or bellows (Ni et al., 2002). The fluid mechanics in an OBR are characterised by three dimensionless numbers: the oscillatory Reynolds number (Re_o) that

describes the intensity of mixing, the Strouhal number (St) that describes the effective eddy propagation and the net flow Reynolds number (Re_n), as defined in Eq.(1) , (2) and (3) respectively.

$$Re_o = \frac{2\pi f x_o \rho D}{\mu} \quad (1)$$

$$St = \frac{D}{4\pi x_o} \quad (2)$$

$$Re_n = \frac{\rho u_n D}{\mu} \quad (3)$$

where f is the oscillation frequency (Hz), x_o the oscillation centre to peak amplitude (m), ρ the fluid density (kg/m^3), D the tube inner diameter (m), μ the fluid viscosity (Pa s) and u_n is the net velocity.

The advantages of an OBR over conventional reactors include: attainment of plug behaviour at relatively low net flow rates, uniform mixing with low fluid shear and capacity to be linearly scaled-up. Recently Abbot et al. (2014) reported the OBC to achieve maximum conversion rates at reduced power consumption, when compared to conventional stirred tank reactors in enzymatic saccharification of alpha-cellulose. Previous work by Phan and Harvey (2010) showed how the width of the RTD (minimisation of the axial dispersion coefficient) in OBR type platforms could be reduced to approximate plug flow by manipulation of the oscillation conditions, namely amplitude and frequency.

In this work, RTDs and axial dispersion coefficients are determined in a continuously operated meso scale oscillatory baffled crystalliser (meso-OBC) using computation fluid dynamics (CFD). The numerical data will be validated against experimentally obtained axial dispersion coefficients.

2. Methodology

2.1. Computational Fluid Dynamics Approach

For this work, the STAR-CCM+ software package by CD-Adapco was used. This is an integrated package with a 3D CAD development tool, meshing capability and Navier-Stokes fluid flow solver. The meso-OBC tube modelled consisted of 30 inter-baffle cells separated by smooth periodic constrictions, as illustrated in Figure 1. The mean internal diameter of the tube is 5 mm, the diameter of the constrictions is 2 mm and the total section length modelled was 390 mm. Preliminary simulations using shorter tube lengths showed that tracer material was lost through the inlet and outlet boundaries due to the oscillatory nature of the flow. For example, material is transported forward through the outlet face but due to the imposition of a Neumann boundary condition, when the flow reverses, there is an error in concentration of tracer advected back into the computational domain, causing inaccuracies in the overall mass balance. To address this problem, a longer tube was considered, providing an increased distance between the tracer injection point and the inlet or outlet boundaries; similarly tracer measurement points are located in the computational domain some distance from the inlet and outlet, to minimise the effects of loss of tracer through these boundaries.

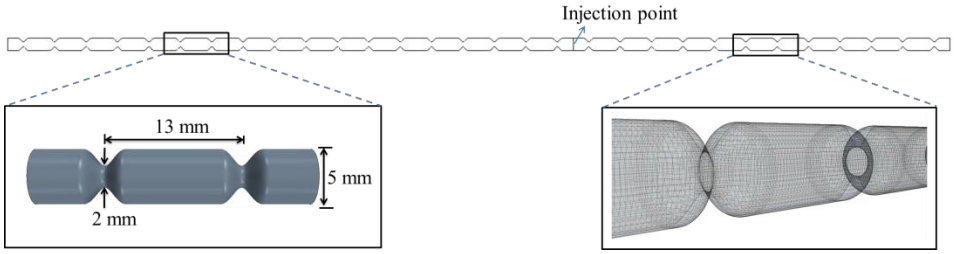

Figure 1: Meso-OBC tube geometry with dimensions, injection point defined and computational mesh

A three dimensional computational grid was generated using a hexahedral mesher (Trimmer mesher in STAR-CCM+), with a high density closer to the walls and baffle constrictions to adequately capture the higher velocity gradients in these regions. A summary of the meshing conditions is shown in Table 1.

Table 1: Mesh conditions

Condition	Specification/value
Mesh type	Trimmer
Cell shape	Hexahedral
Boundary layer	Prism layer mesher
Base size	0.025 mm
No. of computational cells	860,368

Transport equations

The low Reynolds number governing equations for mass continuity Eq.(4), momentum conservation Eq.(5) and the scalar tracer transportation Eq.(6) were solved simultaneously.

$$\nabla . \boldsymbol{u} = 0 \tag{4}$$

$$\rho\left(\frac{\partial \boldsymbol{u}}{\partial t} + \boldsymbol{u} \cdot \nabla \boldsymbol{u}\right) = -\nabla p + \mu \nabla^2 \boldsymbol{u} \tag{5}$$

$$\frac{\partial c}{\partial t} + \boldsymbol{u} \cdot \nabla c = -D_m \nabla^2 c \tag{6}$$

where c is the concentration of tracer, t is the time from the injection of tracer and D_m is the molecular diffusion coefficient of the tracer .

Simulation set up and boundary conditions

Single phase flow in the OBC was modelled in the Eulerian formulation. The model phase was liquid water at 20 °C (998 kg/m^3 and 0.889 mPa s) assumed uncompressible, temporally and spatially-dependent flow. Unsteady inlet boundary conditions were set to represent the time-varying oscillatory flow. The unsteady inlet velocity comprised a net flow rate with an imposed oscillatory flow components defined in Eq.(7).

$$u_{tot} = u_n + 2\pi f x_0 \sin(2\pi f t) \tag{7}$$

Considering the low oscillatory Reynolds numbers (31.3-752) and net flow Reynolds number (8.4 and 21.2), only the laminar flow solver was used for all simulated cases. The convection-diffusion equation Eq.(6) was used to solve the concentration of tracer in time and space.

2.2. Residence time distribution (RTD)

To obtain RTD curves, probes were set at different positions along the pipe downstream of the tracer injection point, within the computational domain. These probes were cross-sectional planes at fixed axial positions i.e. in the middle of successive inter-baffle cells. The measurements were mass flow weighted in order to closely match the so-called 'mixing cup' value that would be measured experimentally.

2.3. Determining axial dispersion

The axial dispersion coefficient is a measure of the degree of spread of an inert trace material along a tubular vessel's longitudinal direction. It is a coefficient that can characterise the degree of back-mixing and quantify the deviation from ideal plug flow behaviour. The quantity is of great interest to the design and operation of tubular reactors, since it can be analysed to determine the residence time distribution of larger or smaller scale vessels of similar geometry.

In order to achieve optimized axial dispersion coefficient values, the RTD curves were fitted to a one-dimensional axial dispersion model.

$$\frac{\partial c}{\partial t} = D_a \frac{\partial^2 c}{\partial x^2} - u_n \frac{\partial c}{\partial x} \tag{8}$$

where x is axial position, D_a is the axial dispersion coefficient and u_n is the mean net velocity.

This procedure applies a parameter estimation method to determine the optimum axial dispersion coefficient and mean net velocity from a transfer function representing the solution to eq.(8) (Zheng et al., 2008, Crittenden et al., 2005) which is convoluted with the measured concentration profile at the first downstream measurement point in order to predict the concentration-time profile of the second measurement point. The output parameters from the model are the mean residence time and the dimensionless dispersion number (D_a/u_nL). The dispersion number represents the overall extent of axial dispersion in the system under consideration and is the reciprocal of the Peclet number ($Pe = u_nL/D_a$). In the dispersion number expression, D_a is the axial dispersion coefficient, u_n is the mean velocity and L is the length between the two measurement points.

3. Results and discussion

A range of conditions were simulated to determine the axial dispersion coefficient exhibited by the meso-OBC. These included net flow rates of 2 ml/min ($Re_n = 8.4$) and 5 ml/min ($Re_n = 21.2$), oscillation frequencies of 2, 6 and 12 Hz and oscillation amplitudes of 0.5, 1 and 2 mm. The computational results presented in Figure. 2 (b) reveal that the narrower RTD are obtained at lower amplitudes, with the narrowest curve achieved at conditions 6 Hz and 0.5 mm. However Figure. 2 (a) does not show a clear relationship between the RTD and the oscillation frequency. This confirms what was reported by Zheng and Mackley, 2008, who proposed a correlation with the Strouhal number (i.e. oscillation amplitude) having a more dominant effect on the axial dispersion than the oscillation frequency.

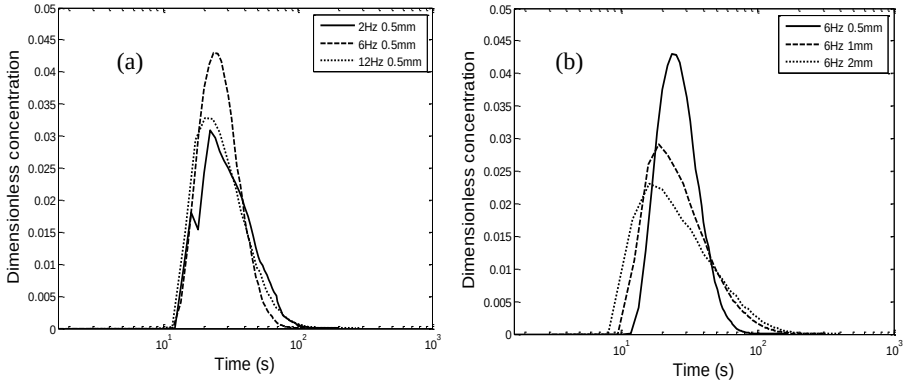

Figure 2. Normalised RTD curves computed at downstream probe 6 (6 interbaffle cells from injection point) for Re_n = 21.2 (a) with increasing oscillatory frequency and (b) with increasing amplitude.

The simulated section was 0.39 m long which is significantly shorter than the tube used in experimental procedures, which precludes direct comparison of the predicted and experimental Peclet numbers. Nevertheless, the axial dispersion coefficients, D_a predicted by CFD are compared to values from Zheng et al (2008), as shown in Figure. 3 (a) at similar values of Re_n and the same oscillatory frequency.

There is an approximately linear relationship between the axial dispersion coefficient and oscillatory Reynolds number at 2 Hz, $Re_n = 8.4$; the axial dispersion coefficient increases with increasing net flow Reynolds number. At the same oscillation frequency, but a higher $Re_n = 21.2$ there is evidence of optimum plug flow conditions being obtained in both the CFD and experimental results, i.e. axial mixing is minimised. At these conditions, eddy formation and detachment generates rapid radial mixing and effectively the device acts as a large number of well-mixed cells in series, with minimal axial dispersion. At the higher oscillation frequency of 6 Hz, $Re_n = 8.4$, the axial dispersion coefficient again increases approximately linearly with increasing net flow Reynolds number.

The results in Figure 3. (b) generally show a decrease in the axial dispersion coefficient with increasing Strouhal number (or decreasing amplitude) for all cases, except for 2 Hz, $Re_n = 21.2$ where an increase in Strouhal number from 0.4 to 0.8 (reduction in amplitude from 1 mm to 0.5 mm) caused an increase in the dispersion coefficient. The explanation for this increase is that because of the higher net flow rate (5ml/min), a very low frequency (2 Hz) should be coupled with a higher amplitude to generate the eddies necessary to increase the radial mixing to a similar order to the axial mixing.

To properly assess the best conditions delivering near plug flow behaviour, the dispersion number, D_a/u_nL needs to be investigated, and the lowest two values were obtained at $Re_o = 31.3$, $St = 0.8$, $Re_n = 8.4$ ($D_a/u_nL = 1.9\times10^{-4}$) and at $Re_o = 94.2$, $St = 0.8$, $Re_n = 21.2$ ($D_a/u_nL = 2.1\times10^{-4}$).

The next stage of this work will be to carry out continuous crystallisation experiments at these low axial dispersion conditions to realise the advantages, if any, are observable in the crystal product size distribution.

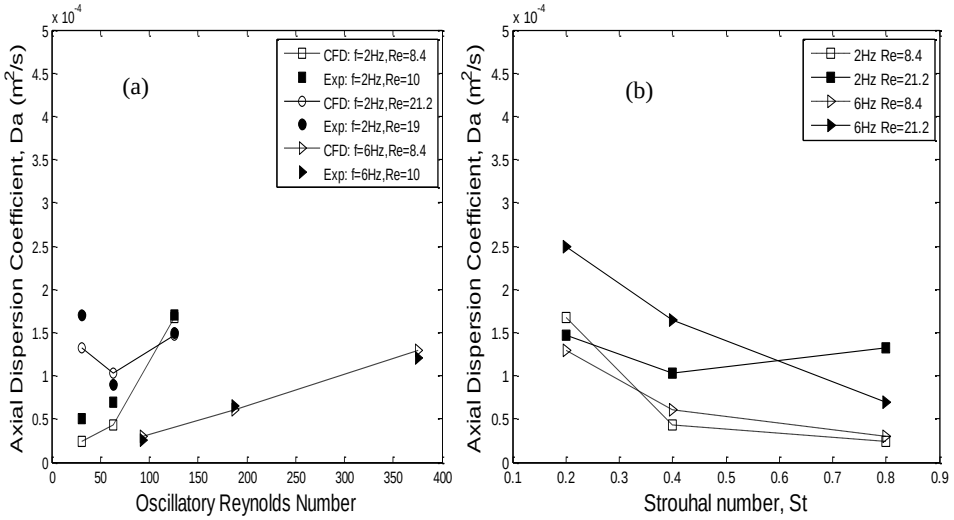

Figure 3. Axial dispersion coefficient as a function of: (a) oscillatory Reynolds number (b) Strouhal number. Experimental data used for validation in (a) was taken from Zheng et al. (2008).

4. Conclusions

A meso-scale oscillatory baffled crystalliser was characterised to determine the best oscillatory conditions that deliver near plug flow behaviour, using a CFD approach. Fine tuning of the oscillations conditions enabled the control of axial dispersion coefficient in the baffled tube due to the increase of the radial mixing. It was found that very low amplitudes (x_o < 1 mm*)* and medium oscillation frequencies (f ~ 6Hz) delivered the narrowest RTD curves and lowest axial dispersion coefficient. The axial dispersion coefficient showed an increase with net flow Reynolds number, Re_n. Fine tuning of oscillation conditions has shown to improve mixing in the meso-OBC evident in the low axial dispersion coefficient range (7×10^{-5} m^2 s^{-1}) obtained at 0.5 mm amplitude and 6 Hz frequency at $Re_n = 21.2$.

References

M. S. R. Abbott, G. Valente Perez, A. P. Harvey, and M. K. Theodorou, 2014, "Reduced power consumption compared to a traditional stirred tank reactor (STR) for enzymatic saccharification of alpha-cellulose using oscillatory baffled reactor (OBR) technology," Chem. Eng. Res. Des., vol. 92, no. 10, pp. 1969–1975.

C. R. Brunold, J. C. B, Hunns, M. R. Mackley and J. W. Thompson, 1989, 'Experimental Observation on Flow Patterns and Energy Losses for Oscillatory Flow in Ducts Containing Sharp Edges', Chem. Eng. Sci., Vol. 44 , No. 5, pp. 1227-1244-1244.

B. D. Crittenden, A. Lau, T. Brinkmann, R.W. Field, 2005, 'Oscillatory flow and axial dispersion in packed beds of spheres', Chemical Engineering Science, Vol. 60, pp. 111-122.

X. Ni, H. Jian, A. W. Fitch, 2002, 'Computational fluid dynamic modelling of flow patterns in an oscillatory baffled column', Chem. Eng. Sci., Vol. 57, 2849-2862

A. N. Phan, A. Harvey, 2010, 'Development and evaluation of novel designs of oscillatory continuous mesoscale oscillatory baffled reactors' , Chem. Eng. J., Vol. 159, pp. 212-219.

M. Zheng and M. Mckley, 2008,'The axial dispersion performance of an oscillatory flow meso-reactor with relevance to continuous flow operation' Chem. Eng. Sci. , Vol. 63, 1788-1799.